Nanometer-Scale Solvent-Assisted Modification of Polymer Surfaces Using the Atomic Force Microscope

R. N. Leach,† F. Stevens,† C. Seiler,‡ S. C. Langford,† and J. T. Dickinson*,†

Physics Department, Washington State University, Pullman, Washington 99164-2814, and FHOOW, Emden, Germany

Received July 16, 2003. In Final Form: September 17, 2003

We describe the response of poly(methyl methacrylate) surfaces to localized mechanical stimulation by the tip of an atomic force microscope (AFM) in water, methanol, ethanol, and aqueous alcohol solutions. Simply pressing the AFM tip into the surface with no horizontal motion fails to produce visible features in subsequent low contact force images. A single small-area (40×40 nm^2) high contact force scan has little effect in air but in water or in alcohol−water mixtures produces soft bumps (local volume increase) adjacent to the scanned area. These bumps typically have lateral dimensions of ∼100 nm and rise tens of nanometers above the surrounding surface. Larger, micron-scale scans produce approximately parallel, raised ridges 50−150 nm apart. These structures are stable over time periods of hours or more in air and in solvent. We present evidence that these modifications are due primarily to stress-enhanced solvent uptake in material surrounding the area of tip−polymer contact.

1. Introduction

With the atomic force microscope (AFM), well-characterized forces can be applied to a surface with nanometer-scale spatial resolution. AFM scanning at low contact forces is often used for nondestructive surface imaging. At higher contact forces, in combination with chemically aggressive environments, scanning can significantly modify many surfaces. Exploiting these effects to control material deposition or removal would allow surfaces to be micromachined. In previous work, we have shown that AFM scanning in appropriate chemical environments can locally modify the surfaces of single-crystal minerals including brushite,[1] calcite,[2,3] and sodium nitrate.[4]

Polymers are soft enough to be modified by hard AFM tips, such as those of silicon nitride, yet rigid enough to hold their shape after modification. The chemical structure of glassy polymers allows for several unique deformation modes and chemical interactions, for example, shear yielding and crazing. Scanning polymer surfaces in solvents or air often produces bumps or raised patches.[5−10] These effects are presumably similar to chemically induced swelling in polymers damaged by controlled scratching.[11] While the effect of varying the scanning time or scanning force has received some study, there have been no reports on the effect of changing the solvent.

In this work, we examine the effect of scanning a common glassy polymer, poly(methyl methacrylate) (PMMA), in air, water, ethanol, methanol, and alcohol−water solutions. Under a wide range of contact forces and solutions, the continuous application of a normal force by the AFM tip does not permanently alter the PMMA surface. However, superimposing a nanometer-scale scanning motion on this normal force produces localized volume increases (bumps/protrusions) in water and alcohol solutions and localized volume decreases (indents) in 100% methanol. Larger, micron-scale scans under similar conditions in alcohol solutions produce sets of parallel ridges roughly perpendicular to the AFM fast-scan direction. We present evidence that these modifications are primarily due to enhanced solvent uptake induced by the stress and motion of the tip at the polymer surface and that for a given solvent there is a threshold in stress to generate material modification.

2. Experiment

Solvents. The solvents employed in this work include deionized water, reagent grade methanol (Fisher), and various mixtures of methanol or ethanol and water. Most ethanol solutions employed an HPLC grade of denatured ethanol (Fisher), containing 90% ethanol, 5% methanol, and 5% 2-propanol. Absolute ethanol (Midwest Grain Products) was employed in a small number of experiments. The effect of substituting denatured ethanol for absolute ethanol was not statistically significant.

Film Preparation. Glass microscope slides (Precleaned Gold Seal Micro Slides from Becton, Dickinson, and Co.) were used as received or were surface treated to improve film adhesion. Surface-treated slides were cleaned by sonication in 1 M NaOH, rinsed with dilute HCl, deionized water, and acetone, and oven dried. The slides were then soaked for 20 min in a 0.014 M solution of 3-(trimethoxysilyl)propyl methacrylate in ethanol. After rinsing with acetone, methyl methacrylate was then polymerized on the surface of the slides, and the slides were rinsed again with acetone. Polymer films deposited on treated glass showed greatly enhanced stability to alcohol and alcohol−water solutions.

Poly(methyl methacrylate) (Aldrich, $M_w \sim 145\,000$ amu) powder was dissolved in a mixture of 67% propylene glycol methyl ether acetate and 33% γ-butyrolactone. (The solution was at about 15% polymer by weight.) A few drops of polymer solution were

* Corresponding author. E-mail: jtd@wsu.edu.
† Washington State University.
‡ FHOOW.

(1) Scudiero, L.; Langford, S. C.; Dickinson, J. T. *Tribol. Lett.* **1999**, *6*, 41−55.
(2) Park, N.-S.; Kim, M.-W.; Langford, S. C.; Dickinson, J. T. *Langmuir* **1996**, *12*, 4599−4604.
(3) Park, N.-S.; Kim, M.-W.; Langford, S. C.; Dickinson, J. T. *J. Appl. Phys.* **1996**, *80*, 2680−2686.
(4) Nakahara, S.; Langford, S. C.; Dickinson, J. T. *Tribol. Lett.* **1995**, *1*, 277−300.
(5) Jin, X.; Unertl, W. N. *Appl. Phys. Lett.* **1992**, *61*, 657−659.
(6) Iwata, F.; Matsumoto, T.; Ogawa, R.; Sasaki, A. *Jpn. J. Appl. Phys., Part 1* **1999**, *38*, 3936−3939.
(7) Iwata, F.; Matsumoto, T.; Ogawa, R.; Sasaki, A. *J. Vac. Sci. Technol., B* **1999**, *17*, 2452−2456.
(8) Zhou, L.; Zhang, P. C.; Ho, P. K. H.; Xu, G. Q.; Li, S. F. Y.; Chan, L. *J. Mater. Sci. Lett.* **1996**, *15*, 2080−2084.
(9) Kaneko, R.; Hamada, E. *Wear* **1993**, *162−164*, 370−377.
(10) Bhushan, B.; Koinkar, V. N. *Tribol. Trans.* **1995**, *38*, 119−127.
(11) Blackman, G. S.; Lin, L.; Matheson, R. R. In *Micro- and Nano-Wear of Polymeric Materials*; Tsukruk, V. V., Wahl, K. J., Eds.; American Chemical Society: Washington, DC, 2000; pp 258−269.

10.1021/la035289n CCC: $25.00
Published on Web 10/25/2003

placed on a soda-lime glass slide, spun at 500−900 rpm for 10−30 s, dried at 95 °C for 1 h, and stored in a desiccator. The resulting films were 5−15 μm thick. Films deposited on both treated and untreated substrates displayed similar root-mean-square (RMS) roughnesses of about 0.3 nm over a 3 × 3 μm^2 area.

Atomic Force Microscopy. Most surface modification experiments were performed with a Molecular Imaging PicoScan AFM in contact mode. Unless otherwise noted, Nanoprobe AFM tips from Digital Instruments from a single wafer were used. These tips are square pyramids of CVD silicon nitride with a tip angle of 70° and a nominal tip radius of curvature of 20−50 nm. Force constants for cantilevers from this same wafer were determined by Asylum Research using thermal noise or reference spring methods. For tapping mode imaging or when stiffer cantilevers were needed, Mac Mode cantilevers (Molecular Imaging) or NSC-11B cantilevers (MikroMasch) were used. Both of these cantilevers employ silicon tips with a cone angle of ∼20°. Mac Mode cantilevers have a hard magnetic cobalt coating and a nominal tip radius of 50 nm. The NSC-11B tips have a nominal tip radius of 10 nm. Force constants for the Mac Mode and NSC-11B cantilevers were estimated from observed resonant frequencies and force constant versus resonant frequency data provided by the manufacturers.

Lateral Force Estimates. The lateral force constant was estimated from the known normal force constant by assuming that $k_{\text{normal}}/k_{\text{lateral}}$ was about 0.0032. This ratio was determined numerically for tips with similar geometry.[12] The lateral detector sensitivity was then estimated from the change in the slope of the friction loop as the tip begins to slide.[13] For measurements in air, the normal force was corrected to include adhesion (measured from the force−displacement curve).[14]

Surface Modification. The majority of the PMMA imaging and modification was done in contact mode. First, the flatness of the surface to be modified was verified with a preliminary 3 × 3 μm^2 scan at low contact force (∼15 nN). The contact force and scan size were then set to values appropriate for surface modification, and a high-force scan was acquired. Most modification was performed at a scan rate of 3.1 lines/s. Finally, a 3 × 3 μm^2 image of the resulting features was acquired at low contact force at 1.12 lines/s. All images consisted of 256 scan lines of 256 data points each, with the fast-scan axis horizontal.

Some AFM imaging was performed in the tapping mode using the Molecular Imaging MAC mode. In the MAC mode, an oscillating magnetic field drives a magnetically coated cantilever near its resonant frequency. The MAC mode can easily be turned off to allow high force contact and then turned back on to allow imaging in the MAC mode.

In all solutions, the polymer surface could be imaged without noticeably altering the surface by scanning at contact forces of 3−20 nN. Force−displacement curves (taken by pressing the tip into the sample and then retracting) could also be acquired without altering the surface, as long as the maximum applied force was less than 20 nN. Force−displacement curves were used to estimate the Young's modulus of both modified and unmodified polymer assuming Hertzian contact.[15]

Volume Change Measurement. Scanning in water and alcohol solutions often produced bumps or indentations in the scanned area. The magnitude of the total change in polymer volume (relative to the surrounding surface plane) was estimated numerically. First, the overall slope of the image outside the modified area was determined from several scan lines along each edge of the image. This 2D slope was then subtracted from the image. The feature of interest was then selected, and a vertical cutoff limit was assigned, corresponding to the minimum significant feature height. A Mathematica program was used to identify the pixels in the selected area whose elevation above or below the surrounding plane was greater than the cutoff. The heights of the selected pixels were summed and multiplied by the area per pixel to obtain the total volume change. Only surface modifications made with the Digital Instruments cantilevers were analyzed for volume and other statistics.

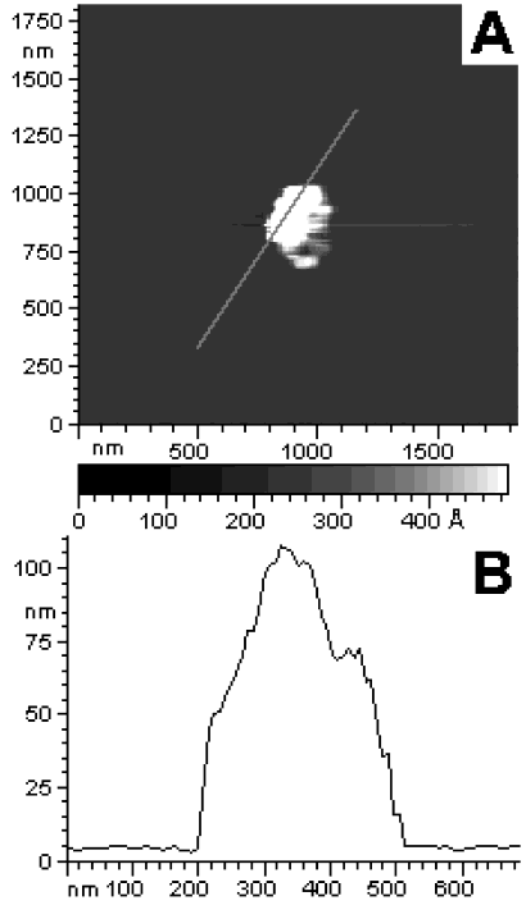

Figure 1. AFM image of a PMMA film scanned in 50% ethanol solution. The central area (40 × 40 nm^2) was scanned once at a normal force of 180 nN, using a 0.36 N/m cantilever. (A) Typical image showing a raised bump; (B) cross section through the bump.

3. Results

Bumps Produced by Small-Area Scanning. In most of the studied solvents, applying a simple normal force with the tip (with no lateral motion) has little effect on the appearance of the surface in subsequent images. However, even modest, cyclic, lateral motion of the tip during the application of force in water or alcohol solutions produces dramatic, localized, elevated regions near the scanned area. The central 40 × 40 nm^2 region of the PMMA surface in Figure 1 was scanned once at a contact force of 180 nN in 50% ethanol solution over a period of 83 s. This treatment produced the protrusion (bump) on the surface, roughly 100 nm high, ∼150 nm full width at half-maximum, with a base diameter of ∼300 nm. The elevation above the surrounding region reflects a net increase in polymer volume. The bump in Figure 1 extends well beyond the area actually contacted by the AFM tip during scanning. Assuming Hertzian contact, applying a force of 180 nN to a spherical stylus with a tip radius of 30 nm generates a circular contact 25 nm in diameter that penetrates 5 nm into the polymer.[16] Despite the non-Hertzian nature of contact, it is unlikely that the tip

(12) Neumeister, J. M.; Ducker, W. A. *Rev. Sci. Instrum.* **1994**, *65*, 2527−2531.
(13) Cain, R. G.; Biggs, S.; Page, N. W. *J. Colloid Interface Sci.* **2000**, *227*, 55−65.
(14) Ando, Y.; Ishikawa, Y.; Kitahara, T. *J. Tribol.* **1995**, *117*, 569−574.
(15) Chizhik, S. A.; Huang, Z.; Gorbunov, V. V.; Myshkin, N. K.; Tsukruk, V. V. *Langmuir* **1998**, *14*, 2606−2609.
(16) Timoshenko, S. P.; Goodier, J. N. *Theory of Elasticity*, 3rd ed.; McGraw-Hill: New York, 1970.

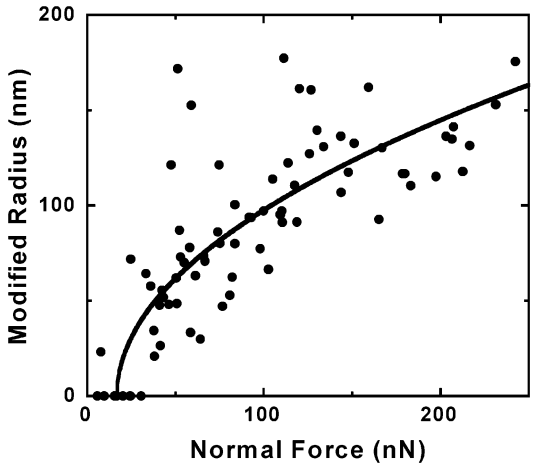

Figure 2. Effective radius of the modified region [$r_{boundary} = (area/\pi)^{1/2}$] versus normal force in 50% ethanol solution, taken with four different cantilevers, $k_{normal} = 0.07-0.41$ N/m. The curve represents the least-squares fit of eq 3 to the data.

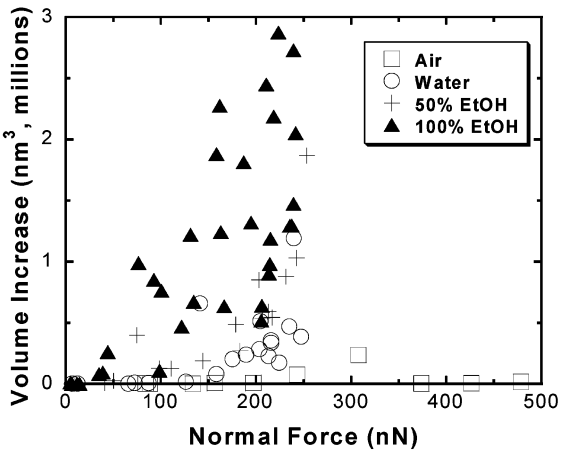

Figure 3. Volume increase produced by 40 × 40 nm² scans in various solutions versus contact force, using a 0.41 N/m cantilever. The higher contact forces in air are due to the contribution of adhesion. Data for 50% methanol (not shown) overlap data for 50% ethanol.

contacted the entire elevated region. This suggests that stresses generated by friction and plowing play a role in bump formation. These stresses extend well beyond the area actually contacted by the tip.

The relatively sharp boundary around the outside edge of the modified region is noteworthy. Since the tip-induced stresses fall gradually with distance from the tip, the sharp boundary suggests that the modification is a strongly nonlinear function of stress. For instance, modification may require stresses above a certain threshold, similar to a yield stress. Increasing the normal force, F_N, systematically increases the size of the bumps. Figure 2 displays the effective radius of the elevated regions (equal to the square root of the bump area, after dividing by π) as a function of F_N for a series of bumps produced in 50% ethanol−water solutions. The data also suggest there is a minimum force below which no feature is created. The dark line is a least-squares fit of a model presented below to these data.

Measurements of the apparent coefficient of friction at low contact forces, where surface modification is absent or minimal, typically yield values of 0.1−0.2 in air and in all solvents except for pure methanol, where the coefficient of friction is somewhat higher, ∼0.3. At contact forces sufficient to modify the surface during scanning, higher coefficients of friction (0.3−0.6) are observed in air and in most solvents. An even higher value of 0.9 is observed in 100% methanol. The friction measurements do not depend on scan size or speed. The increase in the coefficient of friction at the onset of surface modification is likely due to plowing and indicates that the lateral interaction of the tip with the surface is sufficient to produce a strongly anisotropic distribution of stress extending many tens of nanometers away from the tip.

The local volume *increase* produced by a single 40 × 40 nm² scan in air, in water, and in 50% and 100% ethanol solutions is shown as a function of applied normal force in Figure 3. (Volume changes in 50% methanol (not shown) are similar to the volume changes observed in 50% ethanol solution.) In air, volume increases are very small even at normal forces as high as 500 nN. In solution, the change in volume increases with increasing normal force. Compared to scanning in air, pure water clearly shows a volume increase response. In 50% alcohol and pure ethanol, the volume increase can be dramatic at the higher normal forces. At the high end of the normal force range, as seen, variability in the volume change can be considerable.

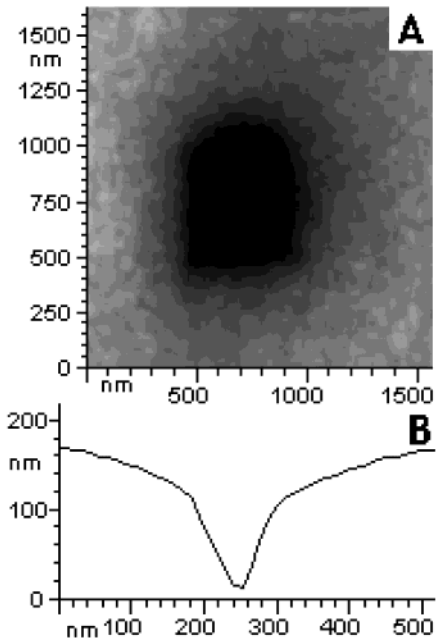

Figure 4. AFM image of a PMMA film scanned in 100% methanol using a 0.41 N/m cantilever. The central 40 × 40 nm² area was scanned once at a normal force of 240 nN. (A) Typical image showing indentation; (B) cross section through the center of the indent.

Scanning in pure methanol also shows a larger effect at higher forces but with a volume decrease.

Indent Formation by Small-Area Scanning in Pure Methanol. In 100% methanol solution, similar 40 × 40 nm² scans produce large depressed regions, rather than bumps, as shown in Figure 4. In contrast to the bumps produced in other solutions, the indents produced in 100% methanol solution can be produced by applying a simple normal force (no lateral motion) and are not stable. The indent volume typically diminishes by almost an order of magnitude during 30 min of low contact force scanning. Further, the boundaries of the indented region lack the sharp edges characteristic of the bumps formed in water and ethanol solutions. This suggests that indent formation is a much less nonlinear function of stress than bump formation.

Modification by Large-Area Scanning. Micron-sized scans acquired under conditions similar to those that

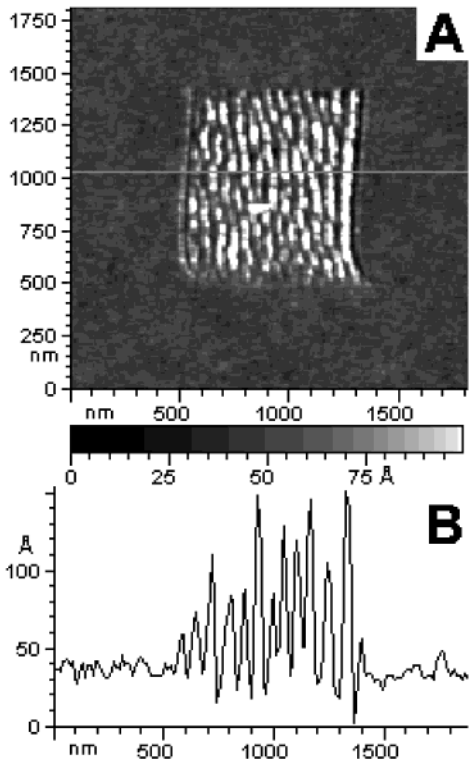

Figure 5. AFM image of a PMMA film scanned in 50% ethanol solution using a cantilever with a force constant of 0.36 N/m. The central 750 × 750 nm^2 area was scanned once at a higher normal force of 180 nN immediately before this image was acquired. (A) Typical AFM image of ridges; (B) horizontal cross section.

produce raised bumps typically produce parallel, raised ridges perpendicular to the horizontal fast-scan direction. Figure 5A is an image of ridge features produced by a single 750-nm scan at a normal force of 180 nN in a 50% ethanol solution. The ridges in Figure 5A are 5−10 nm high, while the valleys between them are only 1−2 nm deep, as shown in Figure 5B. Like the bumps, these ridges reflect a net increase in polymer volume above the surrounding background. In contrast, similar ridge structures on crystalline sodium nitrate were formed by material transfer alone, with no net volume change.[17]

Similar ridge patterns were produced by large-area scanning (>300 × 300 nm^2) in 50% methanol and ethanol solutions at high normal forces, but not in air or in water. The ridge-to-ridge distance varies with solvent, normal force, and scan speed but is typically in the range of 50−150 nm. The ridge-to-ridge distance does not depend on the cantilever force constant. Under a given set of solution and scanning conditions, the formation of well-ordered, periodic ridges is observed only within a relatively narrow range of contact forces. Lower normal forces have little effect on the surface, while higher normal forces heavily modify the surface in a nonperiodic fashion.

Once formed, both ridges and bumps are stable under repeated scanning in solvent at low normal forces. A typical raised area produced in 50% ethanol was scanned for 3.5 h with no significant reduction in height, area, or volume. Ridge formation in previous work (mostly in air) typically required much higher normal forces (100−1000 nN[6,7,18−22]) or prolonged scanning (30−60 min[23−25]). Here, in alcohol solutions, we observe ridge formation after only a *single scan* (for a total scan time of about 1 min) at moderate normal forces of 100−300 nN.

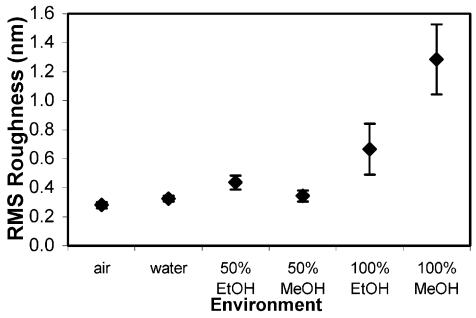

Figure 6. RMS roughness of PMMA films in different solvents. Each data point represents the average and standard deviation of several measurements taken on each of several different samples. Both the average and the scatter increase in the stronger solvents.

Surface Modification by Solvent Alone. Polymers can be strongly affected by solvent exposure even in the absence of applied stress. These effects include solvent swelling (volume increase) and, in strong solvents, dissolution. Given adequate polymer−substrate adhesion, the principle effect of methanol and ethanol solutions in the absence of AFM stimulation is a modest increase in surface roughness. Average roughness values computed from 3 × 3 μm^2 scans in each of the solutions employed in this work appear in Figure 6. Significantly, films exposed to solvent and then dried did not regain their original (low) roughness. The increased roughness persists long after the solvent evaporates, suggesting that the near-surface network of polymer chains is altered irreversibly during solvent exposure.

Stiffness Measurements. Solvent exposure can also soften polymeric materials. Using appropriately stiff cantilevers, the effective Young's modulus of the near-surface material can be determined from the rate of cantilever deflection as the tip is pushed against the surface.[15] Reasonable stiffness measurements require that the cantilever is stiff enough to significantly deform the surface but flexible enough to allow for measurable deflection during the experiment. The relatively stiff MAC mode cantilevers are well suited for measurements on PMMA.

Stiffness measurements were performed by first imaging the surface in the (noncontact) MAC mode. Surface modification was then performed in the contact mode, followed by force curve acquisition (measurements of tip deflection versus tip displacement) to probe the stiffness of modified and nearby unmodified material. Finally, the modified region was again imaged in the MAC (noncontact) mode. Surface modification with the MAC mode cantilevers was performed at higher normal forces (~10 μN) than in the work above with Digital Instruments cantilevers. As a consequence, the bumps produced by small-

(17) Nakahara, S.; Langford, S. C.; Dickinson, J. T. *Tribol. Lett.* **1995**, *1*, 277−300.
(18) Nie, H.-Y.; Motomatsu, M.; Mizutani, W.; Tokumoto, H. *J. Vac. Sci. Technol., B* **1997**, *15*, 1388−1393.
(19) Brumfield, J. C.; Goss, C. A.; Irene, E. A.; Murray, R. W. *Langmuir* **1992**, *8*, 2810−2817.
(20) Elkaakour, Z.; Aimé, J. P. *Phys. Rev. Lett.* **1994**, *73*, 3231−3234.
(21) Leung, O. M.; Goh, M. C. *Science* **1992**, *255*, 64−66.
(22) Hamada, E.; Kaneko, R. *Ultramicroscopy* **1992**, *42−44*, 184−190.
(23) Meyers, G. F.; DeKoven, B. M.; Seitz, J. T. *Langmuir* **1992**, *8*, 2330−2335.
(24) Nick, L.; Kindermann, A.; Fuhrmann, J. *Colloid Polym. Sci.* **1994**, *272*, 367−271.
(25) Jing, J.; Henricksen, P. N.; Wang, H.; Marteny, P. *J. Mater. Sci.* **1995**, *30*, 5700−5704.

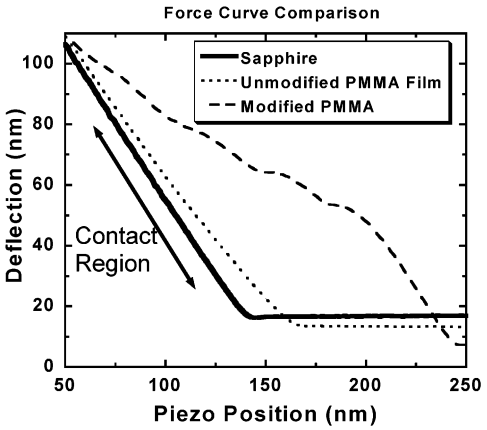

Figure 7. Approach portion of force curves on three surfaces, acquired with a cantilever with a spring constant of 93 N/m. The solid line on the left was taken on sapphire and represents the response of an extremely stiff substrate. The dotted line was acquired on an otherwise unmodified PMMA film in 60% ethanol solution; the lower slope reflects the softness of PMMA in this solvent. The dashed line was acquired on a modified area of the PMMA film; the much lower slope indicates that the modified material is a great deal softer than the unmodified PMMA.

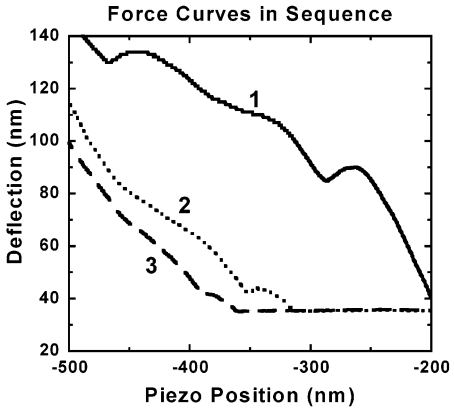

Figure 8. Three force curves taken sequentially at the same position on a modified region of PMMA in 60% ethanol solution using a cantilever with a spring constant of 2.8 N/m. The slope of the contact region becomes steeper with each force curve acquisition, suggesting that the material beneath the tip is getting harder.

area scanning in the contact mode with MAC mode cantilevers were much larger than those done with lighter cantilevers. From a given force curve, we obtained the modulus using the analysis provided by Chizhik et al.[15]

$$E_j = \frac{3}{4}(1-\nu^2)\frac{k_n z_{defl}}{R^{1/2}h^{3/2}} \quad (1)$$

where E_j is the stiffness (Young's modulus) at point j of the force curve, in Pa; ν = Poisson's ratio (taken as 0.33 for PMMA); k_n is the spring constant of the AFM cantilever, in N/m (∼93 N/m for the MAC mode cantilevers employed in stiffness measurements); z_{defl} is the deflection of the AFM cantilever, in nm; R is the radius of curvature of the AFM tip, in nm; and h is the distance the AFM tip penetrates the surface, in nm.

Applying this analysis to unmodified PMMA films in air yields an effective modulus of 2.5 GPa in air. Published values of Young's modulus for bulk PMMA typically range from 2.5 to 5.0 GPa,[26−28] consistent with this result.

Figure 7 shows force curves acquired with MAC mode cantilevers on a hard reference material (sapphire, solid line), an unmodified PMMA surface in 60% ethanol (dotted line), and a surface modified by one small-area scan in 60% ethanol using a contact force of 25 μN (dashed line). The slope in the contact region is slightly reduced in 60% ethanol and is greatly reduced and irregular in the modified region. The slope of the force curves corresponds to an effective modulus of 0.76 GPa in the 60% ethanol solution. The low-slope portion of the force curve on modified material corresponds to a modulus of about 0.01 GPa; this value most likely reflects material properties very near the polymer−solvent interface, where one expects the highest concentration of absorbed solvent. Although the effective modulus of the modified material varies markedly from point to point, the modified material is dramatically softer than PMMA in air or in ethanol solution before modification. This reduction in modulus may play an important role in the deformation process leading to bump formation.

Although the bumps are quite robust under prolonged, low contact force scanning (∼15 nN), they can be modified by using higher forces or by bringing the AFM tip down vertically onto the surface for a stiffness measurement. Figure 8 shows three force curves taken sequentially at one point on a modified polymer surface using a Digital Instruments cantilever (spring constant ∼ 2.8 N/m). The modification was produced by a single small-area scan at a contact force of 650 nN. With each successive force curve acquisition, the point of tip−polymer contact (as indicated by the onset of cantilever deflection) moves downward (to the left in Figure 8) and the slope of the force curve grows steeper. Much of the local volume increase produced by small-area scanning is lost during force curve acquisition, and much of the lost stiffness is restored. Subsequent imaging showed no clear evidence of surface damage (e.g., wearlike features). The modified areas were rough enough that small changes at the point where force curves were taken would have been difficult to observe.

Dye Absorption. The raised bumps and ridges produced during scanning suggest that solvent molecules are incorporated into the near-surface material. This hypothesis can be tested directly by adding a fluorescent dye to the solvent. Surface regions with incorporated dye molecules can then be imaged by dye fluorescence. We performed tip-induced modification experiments in a 0.01 M solution of Rhodamine 6G laser dye (Lambda Physik) in a 50% ethanol solution. For ease of optical imaging, larger AFM scans of ∼15 μm were used. After scanning, these samples were rinsed with a 50% ethanol solution to remove any residual dye, dried, and mounted on the stage of an optical microscope. The dye fluorescence was excited with 248-nm radiation from a Lambda Physik, Lextra 200 excimer laser (KrF) and imaged through an optical microscope with a CCD camera. Figure 9 shows an optical fluorescence image of a PMMA surface modified by multiple AFM scans under dye solution. The scanned regions appear as bright fluorescent patches, showing that solvent and dye have been incorporated into the scanned areas. The incorporated dye was not removed during the rinsing process, suggesting that dye patches produced by this method are stable. The presence of Rhodamine 6G molecules (M_w = 479) implies that the smaller solvent molecules are also incorporated into modified material.

(26) Briscoe, B. J.; Sebastian, K. S. *Proc. R. Soc. London, Ser. A* **1996**, *452*, 439−457.
(27) Marshall, G. P.; Coutts, L. H.; Williams, J. G. *J. Mater. Sci.* **1974**, *9*, 1409−1419.
(28) Brandrup, J.; Immergut, E. H.; Grulke, E. A. *Polymer Handbook*; Wiley: New York, 1999.

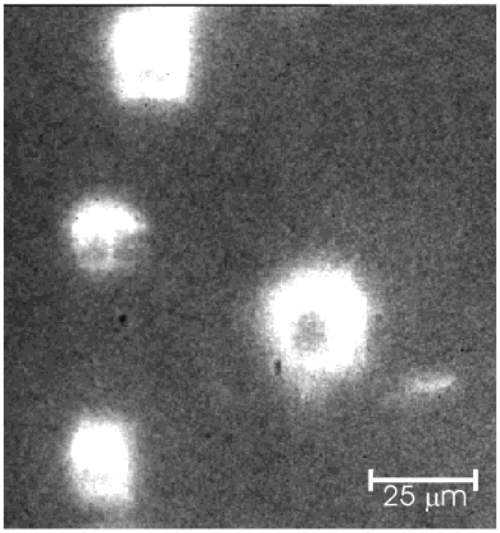

Figure 9. Fluorescence image of a PMMA surface after several $15 \times 15\ \mu m^2$ AFM scans performed in a 0.01 M solution of Rhodamine 6G dye in 50% ethanol solution. Illumination is with UV light at 248 nm. The bright areas correspond to surface patches with high concentrations of dye. Under white light illumination, no contrast was observed between the scanned regions and the surrounding surface.

The volume change in modified material is accompanied by significantly enhanced solvent uptake.

4. Discussion

Solvent alone causes only a general roughening of the polymer surface (Figure 6). Stress alone causes only very small changes to the polymer surface (Figure 3, air). Solvent and stress together are required to cause large changes to the polymer surface, and the changes occur at and near the location where the stress is applied. The bumps and ridges described above are formed by the synergistic action of mechanical stress and chemical effects. The localized stress applied by the AFM tip is responsible for the localization of the resulting surface features. Further, the oscillating, back-and-forth nature of tip motion appears to be necessary for the volume increase associated with bump and ridge formation.

Bump Formation. The formation of raised patches of surface during small-area scanning, but not pure normal loading, indicates that static stresses are not sufficient for bump formation. In other materials systems, static stresses can strongly enhance material−solvent interactions. In single-crystal calcite, normal loading by the AFM tip can locally enhance the dissolution rate and produce localized indentations near the point of contact.[3] In contrast, bump formation in PMMA requires *motion* of the tip. With $40 \times 40\ nm^2$ scans and high contact forces (>50 nN), it is likely that the motion of the tip is primarily a rocking motion, with perhaps a small amount of slip. We consider this cyclic nature of the lateral motion during small-area scanning to be very important in generating the localized net increase in polymer volume, presumably accompanying the diffusion of solvent into the polymer.

Solvent swelling, where the volume of a glassy polymer increases when immersed in a suitable solvent, is a well-studied phenomenon. Measurements of solvent swelling in thin films similar to those employed in this work suggest that several days are required to attain quasistatic equilibrium in 50% alcohol solutions.[29] We have found that bumps produced on equilibrated thin films are similar to features produced on films newly exposed to solvent. Since equilibrated films are not expected to take up additional solvent, the local solvent concentration in the bumps and ridges must exceed quasistatic equilibrium values. The applied stresses are *enhancing* solvent uptake.

We envision that the volume of polymer modified by AFM/solvent stimulation extends well into the bulk, below the scanned region. Although we cannot measure the thickness of the modified layer, a reasonable upper bound is given by the horizontal extent of the modified region at the surface. The modified region in Figure 1 is approximately $200 \times 200\ nm^2$ at the surface. If the modified material extends 200 nm into the bulk, the observed volume change of $0.4 \times 10^6\ nm^3$ corresponds to an average 5% increase in volume. Since this is an average value, we expect that local fractional volume changes may be significantly higher.

Polymers are typically softened by the introduction of solvent molecules, and this is indeed observed. The stiffness of films immersed in solvent but not mechanically treated is much less than that of films observed in air (Figure 7). Polymer that has been mechanically treated in the presence of solvent is even softer; the effective modulus is lowered by almost 2 orders of magnitude. These soft structures are not robust when repetitively probed at high contact forces ($\sim 10\ \mu N$) during force curve acquisition (Figure 8). All these mechanical properties are consistent with a high volume fraction of solvent. It is perhaps remarkable that these features are so persistent, being virtually unchanged by hours of low contact force scanning in solution.

In ethanol, water, and alcohol−water solutions, the PMMA film becomes easier to modify but remains rigid, as shown by the fact that the bumps are stable once made. Macroscopically, PMMA is much more readily swelled by methanol than by water or ethanol,[29] and methanol also has a much greater effect on film properties. In pure methanol, the surface roughness increases significantly (Figure 6), and the polymer is softened to a much larger extent than in the other solvents, causing it to lose its rigidity and become viscoelastic. In contrast to the stable bumps formed in other solutions, the depressions formed in methanol can be made without lateral scanning and relax over tens of minutes. "Bumps" are sometimes formed after high force scans in 100% methanol, but they are difficult to study, as they form at the bottom of the indents.

The incorporation of solvent into the polymer is further supported by the introduction of dye molecules by large-area scanning, which also produces raised patches of polymer. The Rhodamine 6G molecule is quite large ($M_w = 479$). That a molecule of this size can enter the polymer matrix, or at least become entangled in the network, is strong evidence for dramatic modification of the near-surface polymer network.

The introduction of solvent molecules into the polymer requires the presence of a suitable void network. Void-to-void transport often requires the motion of intervening polymer segments. Both void size and segment motion increase under tensile stress, increasing both solvent solubility and mobility. Conversely, void size and segment mobility decrease under compressive stress, reducing solvent solubility and mobility.[30,31] On short time scales, the low solvent mobility in compression will hinder the

(29) Stevens, F. *J. Appl. Polym. Sci.*, submitted.

(30) More, A. P.; Donald, A. M.; Henderson, A. *Polymer* **1992**, *33*, 3759−3761.

(31) Budtova, T.; Suleimenov, I. *Polymer* **1997**, *38*, 5947−5952.

escape of solvent introduced in previous tension cycles. We therefore propose that the net effect of cyclic loading is strongly enhanced solvent uptake.

Solvent uptake is limited principally by the time required for segment motion in the polymer chains. The equilibrium state of the system in the presence of a suitable solvent is a polymer−solvent solution (i.e., total dissolution). Methanol, ethanol, and water are poor solvents for PMMA. In these solvents, a quasistatic equilibrium is gradually reached where compressive stresses generated by persistent entanglements oppose further solvent uptake. This balance is tenuous in the sense that solvent molecules enhance segment mobility. Increasing the concentration of solvent in the polymer can enhance further solvent uptake. This effect can be dramatic if, for instance, a previously hindered class of segment motions becomes possible. The nonlinear interaction of solvent, stress, and polymer explains the large variations in volume change observed at high contact forces and solvent concentrations.

One barrier to complete dissolution is the presence of physical entanglements among the polymer chains. To remove these entanglements, the polymer chains must either break or slide freely along their length (reptation). The time and energy required for these processes provide strong limits on solvent uptake in this work. These entanglements prevent major material displacement and thus prevent the volume decrease one might expect when pushing down on a soft surface with a stiff AFM tip.

The tensile and compressive stresses responsible for bump and ridge formation are associated with the lateral forces generated by the tip. These stresses are highest along the direction of tip motion (parallel to the fast-scan direction), with compressive stresses in front of the tip and tensile stresses behind. In contrast, the stresses in material to either side of the scanned area (along the slow-scan direction) are principally shear and have little effect on solvent solubility and transport. Similarly, the compressive stresses directly under the tip hinder solvent incorporation there.

The stability of the bumps produced by small-area scanning suggests that the diffusion of solvent molecules out of the raised areas is limited or that the polymer network has rearranged to a new configuration. The interaction of a good solvent with a polymer is typically quite similar to the interaction of polymer chains with their neighbors. These chemical forces strongly hinder diffusion out of the network. In typical swollen polymers, the same compressive stresses that limit solvent uptake also drive solvent out by diffusion when the solution is removed. The stability of the bumps and ridges observed in this work is strong evidence that these stresses are to a large degree removed, which implies a significant degree of chain rearrangement.

We attribute the initial stages of bump formation to enhanced solvent incorporation into near-surface material as a consequence of stress-induced polymer segment motion. As solvent molecules enter the polymer network, the plasticizing effect of the solvent further enhances polymer segment motion, eventually resulting in a dramatic increase in the rate of solvent uptake. Prolonged mechanical oscillation raises the local solvent concentration adjacent to the tip well above concentrations that can be obtained in the absence of mechanical stress, accounting for our ability to produce bumps on solvent-saturated thin films.

One open question is the size of the network voids occupied by the solvent and dye molecules in this work. The possibilities span the range from the size of single solvent molecules to sizes more appropriately described in terms of microcrazes. Our dye study (Figure 9) suggests that the voids can contain at least one dye molecule, and voids large enough to incorporate Rhodamine 6G molecules could easily hold tens of ethanol molecules or hundreds of water molecules.

Stress Threshold. The possibility of a threshold in stress required to initiate enhanced swelling is strongly suggested by Figure 2. At points well away from the area of tip contact, the maximum tensile stress along the surface, σ, of a typical spherical indenter versus distance from the center of the contact, r, can be written:[16]

$$\sigma = \frac{(1 - 2\nu)F_N}{2\pi r^2} \tag{2}$$

If we associate the value of r at the boundary ($r_{boundary}$) of the modified region with the threshold stress for modification, $\sigma_{threshold}$,

$$r_{boundary} = \left(\frac{(1 - 2\nu)F_N}{2\pi\sigma_{threshold}}\right)^{1/2} \tag{3}$$

The data typically also show evidence for a minimum normal force, below which no modification occurs (F_{min}). This minimum force is consistent with the expectation that the threshold stress be exceeded in the region *outside* the area of tip−substrate contact. High stresses in the contact area do not contribute to modification. When this threshold normal force is incorporated in eq 3, the relationship between F_N and $r_{boundary}$ becomes

$$\text{for } F_N < F_{min}: \quad r_{boundary} = 0 \quad \text{(i.e., no modification)}$$
$$\text{for } F_N > F_{min}: r_{boundary} = A(F_N - F_{min})^{1/2} \tag{4}$$

where $A = [(1 - 2\nu)^{1/2}(2\pi\sigma_{threshold})^{-1/2}]$ and $\nu \approx 0.33$ for PMMA. Figure 2 shows that this model fits the data. The fit yields values of $F_{min} = 17$ nN and $A = 11$ nm GPa$^{-1/2}$. The best fit value of A corresponds to $\sigma_{threshold} \sim 500$ kPa for this solution.

F_{min} can be used to generate an independent estimate of the critical stress for material modification. At F_{min} (17 nN), the tensile stress along the circle of tip−substrate contact, σ_{edge}, presumably equals $\sigma_{threshold}$. σ_{edge} can be estimated from the Hertz relation for an infinitely stiff, spherical tip:[16]

$$\sigma_{edge} = \frac{(1 - 2\nu)}{\pi}\left[\frac{2F_{min}E^2}{9(1 - \nu^2)^2 r^2}\right]^{1/3} \tag{5}$$

The tip radius of curvature, r, is nominally 40 nN for the Si_3N_4 tips used in this work; Poisson's ratio, ν, is ≈0.33. For Young's modulus, E, we use the low value of $E \approx 0.01$ GPa obtained on modified material because this reflects the material behavior at the polymer−solvent interface. These values yield $\sigma_{edge} \approx 700$ kPa, which is in reasonable agreement with $\sigma_{threshold} \approx 500$ kPa as determined from the fit to the $r_{boundary}$ data. We therefore conclude that there is threshold stress for the observed tip-induced polymer modification.

Ridge Formation. Polymers which have been observed to form ridges similar to those shown in Figure 5 during AFM scanning include polystyrene,[6,7,21,23,32] poly(ethylene oxide),[18] poly(phenylene oxide),[19] polyester,[25] poly(ethylene terephthalate),[10,33] polycarbonate,[22,34] poly(methyl meth-

acrylate),[19,22] polyacetylene,[20] polymer blends,[35] and block copolymers.[24,36] Similar ridges have also been observed on nonpolymeric materials, including proteins on mica,[37] phthalocyanine films,[38] and hydrated sodium nitrate.[4] Nearly all of the previous work was performed in air under ambient conditions, although ridges have been formed in aqueous solutions[32,33] and in acetonitrile.[19] Ridges have been produced in an argon atmosphere to *exclude* water and oxygen.[20] In one case, polystyrene was successfully modified in air but not in water.[21] No previous reports have compared the influence of solution composition on ridge formation.

Ridge formation on PMMA in alcohol solutions cannot be attributed to resonant oscillations in the AFM tip. At the scan sizes and speeds employed in most of this work, the cantilever typically encounters 10−30 ridges per second (10−30 Hz), far below the resonant frequencies of the cantilevers (10−40 kHz). Further, cantilevers with dramatically different force constants (and different resonant frequencies) produce ridges with identical spacing. Conversely, the ridge spacing depends on the solvent composition, which has little effect on cantilever resonances. Finally, the ridge spacing depends strongly on applied force but only weakly on scan speed. Thus, ridge formation is largely independent of the mechanical properties of the cantilever.

The ridge spacing decreases slightly with increasing scan speed and plateaus at scan speeds above 4.5 μm/s. Elkaakour and Aimé observed a similar trend in ridge spacing versus scan speed on polyacetylene, where the ridge spacing plateaus at scan speeds above $\sim$5 μm/s.[20] This is consistent with a mechanism where polymer builds up in front of the AFM tip until the polymer offers enough resistance that the tip is forced to hop over it; along a given scan line, this process repeats itself in a periodic fashion. On the next scan line, the uplifted material from the previous scan line encourages the tip to lift, thus amplifying the effect. After a few scan lines, a ridge or "mogul" forms.[4] The faster the tip moves, the less time the polymer has to relax or move out of the way, and the faster resistance to tip movement builds up. Similar mechanisms have been proposed by other workers.[19,20,23,33,36]

The above discussion of bump formation suggests that ridge formation in large-area scans is associated with the tensile stress field behind the moving AFM tip. This volume increase is facilitated by the presence of appropriate solvents, where ridges can be observed after a single scan. In these solutions, solvent is incorporated into the polymer. Stiffness measurements show that the modified material is much more compliant, which is itself sufficient to generate an instability in tip motion. The tip penetrates softer material more deeply and thus experiences higher lateral forces there. This in turn makes the nearby material even softer. The resulting buildup of lateral force cannot be sustained indefinitely. The tip must eventually rise out of the modified material, producing a patch of less modified material, that is, the trenches between the ridges. With each subsequent pass of the tip, the pattern of soft, more modified material and hard, less modified material is reinforced.

5. Conclusion

The presence of solvent makes poly(methyl methacrylate) surfaces much easier to modify by atomic force microscopy. Small-area scanning at moderate to high contact forces in a variety of alcohol−water solutions produces localized patches of elevated material adjacent to the scanned region. Features as small as 100 nm can be created in this way. In water and ethanol solutions, the volume increase produced is stable over periods of hours or more both in solvent and in air. In 100% methanol, indents can be produced in the surface; this deformation relaxes over periods of tens of minutes. Larger scans with appropriate contact forces and solutions produce parallel ridges of raised material in the scanned area. These ridges are also stable over periods of at least hours. We attribute the raised material to partial disentanglement of the polymer, accompanied by enhanced solvent incorporation into voids. These processes depend strongly on solvent composition as well as the stress applied by the AFM tip; indeed, there is a threshold in stress to generate this modified material.

Stable regions of raised material with lateral dimensions of about 100 nm are readily produced by scanning in solution. Careful choice of solution composition provides considerable control over the scanning parameters required for surface modification. The scanning duration and contact force required for ridge formation in particular are much less in solvent solutions than in air, making surface modification by AFM a more efficient operation. By showing that fluorescent dye molecules dissolved in the solvent can be made to penetrate into the polymer, we have demonstrated that enhanced solvent uptake indeed occurs. In principle, this top-down method of using stress to locally "inoculate" the surface could be exploited to introduce nanometer-scale patches of a number of molecules. Such techniques should be useful in areas such as information storage, nanosensors, chemical species biodetectors, and other technologies.

Acknowledgment. This work was supported by the National Science Foundation under Grants CMS-98-00230, CMS-01-16196, and CHE-02-34726, and a subcontract with the University of Florida as part of a KDI-NSF Collaboration, Grant DMR-99-80015. One of us (R.N.L.) thanks the Ed and Virginia Donaldson Undergraduate Surface Science Research Fund for financial assistance.

LA035289N

(32) Pickering, J. P.; Vansco, G. J. *Appl. Surf. Sci.* **1999**, *148*, 147−154.
(33) Ling, J. S. G.; Leggett, G. J.; Murray, A. J. *Polymer* **1998**, *39*, 5913−5921.
(34) Khurshudov, A.; Kato, K. *Wear* **1997**, *205*, 1−10.
(35) Nie, H.-Y.; Motomatsu, M.; Mizutani, W.; Tokumoto, H. *J. Vac. Sci. Technol., B* **1995**, *13*, 1163−1166.
(36) Maas, J. H.; Stuart, M. A. C.; Fleer, G. J. *Thin Solid Films* **2000**, *358*, 234−240.
(37) Lea, A. S.; Pungor, A.; Hlady, V.; Andrade, J. D.; Herron, J. N.; Voss, E. W. *Langmuir* **1992**, *8*, 68−73.
(38) Bourgoin, J. P.; Sudiwala, R. V.; Palacin, S. *J. Vac. Sci. Technol., B* **1996**, *14*, 3381−3385.